Heliyon 10 (2024) e22972

Contents lists available at ScienceDirect

Heliyon

journal homepage: www.cell.com/heliyon

Unveiling the therapeutic potential: Evaluation of anti-inflammatory and antineoplastic activity of *Magnolia champaca* Linn's stem bark isolate through molecular docking insights

Md. Mahadi Hasan [a], Md. Ekramul Islam [a], Md. Sanowar Hossain [b], Masuma Akter [a], Md. Aziz Abdur Rahman [a], Mohsin Kazi [c], Shahzeb Khan [d], Mst. Shahnaj Parvin [a,*]

[a] *Department of Pharmacy, University of Rajshahi, Rajshahi 6205, Bangladesh*
[b] *Department of Pharmacy, Pabna University of Science and Technology, Pabna 6600, Bangladesh*
[c] *Department of Pharmaceutics, College of Pharmacy, King Saud University, P.O. Box 2457, Riyadh, 11451, Saudi Arabia*
[d] *Center of Pharmaceutical Engineering Sciences, School of Pharmacy and Medical Sciences, University of Bradford, BD7, 1DP, UK*

ARTICLE INFO

Keywords:
Anti-inflammatory
Antineoplastic
Magnolia champaca
Compound isolation
Trans-syringin
Topoisomerase-II
COX-2
Molecular docking
^{1}H-NMR
^{13}C-NMR

ABSTRACT

Magnolia champaca Linn. has traditionally been used for medicinal activity in Asia for treating various chronic diseases as well as a source of food, medicines, and other commodities. Due to the long-used history of this plant, the present study was designed to explore the *in vitro*, *in vivo* and in silico anti-inflammatory and antineoplastic properties of the methanolic extract and fractions and the pure compound isolated from the most active chloroform fraction (CHF) of the stem bark of the plant. The isolated compound from the most active CHF was characterized and identified as a glycoside, trans-syringin, through chromatographic and spectroscopic (^{1}H-NMR and ^{13}C-NMR) analyses. In the *in vitro* anti-inflammatory assay, CHF was most effective in inhibiting inflammation and hemolysis of RBCs by 73.91 ± 1.70% and 75.92 ± 0.14%, respectively, induced by heat and hypotonicity compared to standard acetylsalicylic acid. In the egg albumin denaturation assay, CME and CHF showed the highest inhibition by 56.25 ± 0.82% and 65.82 ± 3.52%, respectively, contrasted with acetylsalicylic acid by 80.14 ± 2.44%. In an *in vivo* anti-inflammatory assay, statistically significant ($p < 0.05$) decreases in the parameters of inflammation, such as paw edema, leukocyte migration and vascular permeability, were recorded in a dose-dependent manner in the treated groups. In the antineoplastic assay, 45.26 ± 2.24% and 68.31 ± 3.26% inhibition of tumor cell growth for pure compound were observed compared to 73.26 ± 3.41% for standard vincristine. Apoptotic morphologic alterations, such as membrane and nuclear condensation and fragmentation, were also found in EAC cells after treatment with the isolated bioactive pure compound. Such treatment also reversed the increased WBC count and decreased RBC count to normal values compared to the untreated EAC cell-bearing mice and the standard vincristine-treated mice. Subsequently, in silico molecular docking studies substantiated the current findings, and the isolated pure compound and standard vincristine exhibited −6.4 kcal/mol and −7.3 kcal/mol binding affinities with topoisomerase-II. Additionally, isolated pure compound and standard diclofenac showed −8.2 kcal/mol and −7.6 kcal/mol binding affinities with the COX-2 enzyme, respectively. The analysis of this research suggests that the isolated

* Corresponding author.
E-mail addresses: mkazi@ksu.edu.sa (M. Kazi), S.khan131@bradford.ac.uk (S. Khan), shahnaj_parvin@ru.ac.bd (Mst.S. Parvin).

https://doi.org/10.1016/j.heliyon.2023.e22972
Received 15 August 2023; Received in revised form 22 November 2023; Accepted 22 November 2023
Available online 3 December 2023

bioactive pure compound possesses moderate to potent anti-inflammatory and antineoplastic activity and justifies the traditional uses of the stem bark of *M. champaca*. However, further investigations are necessary to analyze its bioactivity, proper mechanism of action and clinical trials for the revelation of new drug formulations.

1. Introduction

Inflammation is mainly mediated by reactive chemical species to protect cells from harmful and injurious stimuli and to accelerate the healing process [1]. However, inflammation of cellular components, such as the cell membrane, mitochondria, and DNA, can contribute to the pathogenesis of several chronic diseases, such as neurodegenerative disorders, including memory impairment, Alzheimer's disease, Parkinson's disease, dementia and other diseases, including cancer, diabetes, aging and cardiovascular diseases [2,3]. Therefore, several studies have focused on the development of different drugs to combat inflammatory damage to cellular components, but the effectiveness and side effects of the existing drugs are still major concerns [4]. Proteins play a critical role in maintaining the structural and functional integrity of cells and their intracellular components. When proteins undergo denaturation, they lose their native conformation, and this structural alteration is closely linked to the initiation and perpetuation of inflammation [5]. Inflammation often leads to the release of enzymes such as phospholipase A2, which can degrade cell membranes by breaking down phospholipids. Consequently, cellular contents are released, leading to tissue damage and inflammation. Inhibition of protein denaturation is a key indicator of anti-inflammatory potential. Membrane stabilization assays are employed to assess the ability of a substance to protect and stabilize cell membranes. The egg albumin denaturation assay is used to evaluate the ability of compounds to inhibit the denaturation of proteins. Therefore, compounds or drugs that demonstrate the ability to inhibit protein denaturation are considered potentially valuable for their anti-inflammatory activity.

Another potential health issue for people around the world is neoplasm or cancer, which is responsible for approximately 10 million deaths per year and is one of the major causes of human death [6]. Neoplasm is mainly due to damage to the genetic sequence in the cell by reactive species that results in the uncontrolled proliferation of cells [7]. Reactive species can be formed in the body by nonenzymatic reactions of oxygen with organic compounds as well as by ionizing reactions [8]. Neutralization of reactive oxygen or hydrogen species by compounds with antioxidant properties is well known to protect cellular components and prevent chronic diseases such as neoplasms or cancer [9]. Researchers have found thousands of compounds to combat such damage and diseases, but the scarcity of safe, effective and target-specific therapies is the prime reason for the failure of cancer treatment, which contributes to such a large number of deaths [10–12]. Therefore, the search for any potential compound that will be safe and effective in cancer treatment is still a major focus of biological research.

Nature is always the predominant source of compounds used in therapies and has long been investigated by the scientific community [11,13]. *Magnolia champaca* Linn. is used in Asian countries as a traditional medicinal plant that belongs to the Magnoliaceae family and has been used for the treatment and cure of several diseases, such as diarrhea, common cold symptoms, hypertension, gastric disorder and dyspepsia, fever, rheumatism and pain, abscesses and infections, dysmenorrhea and inflammation [14,15]. The plant has been investigated by researchers, especially the bark, for its antioxidant, antimicrobial, and hypoglycemic activities [16], but no significant study has evaluated the anti-inflammatory or antineoplastic potential of the stem bark part of the plant, nor has any active compound responsible for such activity been reported from the plant part.

Molecular docking is an efficient and cost-effective approach for developing and testing pharmaceuticals. It is a crucial tool in characterizing the interactions between plant phytochemicals (ligand molecules) and various proteins (receptors or target molecules) at an atomic level to determine the binding potential of ligands at target binding sites. The ligands identified by molecular docking can be used for further drug development. In a recent study, topoisomerase II was used as the target protein for antineoplastic studies, while cox2 was used for anti-inflammatory studies [17].

The objective of this study was to investigate the anti-inflammatory properties of the methanolic extract and fractions of stem bark using an *in vitro* method. The study also aimed to identify the active compound responsible for the anti-inflammatory activity by performing chromatographic analysis (TLC, column chromatography and NMR) and evaluating its effectiveness against inflammation and cancer. Additionally, the study included in silico molecular docking to determine the binding capacity of the active compound with its receptor molecules, which could lead to the development of new drug formulations.

2. Materials and methods

2.1. Chemicals and reagents

DAPI (4,6-diamidino-2-phenylindole), trypan blue, acetyl salicylic acid, disodium hydrogen phosphate, sodium chloride, iodine, vanillin, sulfuric acid, vincristine, sodium oxalate, carrageenan, diclofenac sodium, EDTA, Evans blue and acetic acid were purchased from Sigma–Aldrich, MO, USA. Methanol, ethyl acetate, chloroform, *n*-hexane, acetone and sodium phosphate were purchased from Merck, India. The other chemicals and reagents needed in the experiments were of analytical grade and purchased from Sigma–Aldrich and Roche.

2.2. Plant material, preparation of the extract and methodology flow diagram

M. champaca stem bark was collected from the University of Rajshahi campus in November 2018. The plant was authenticated by the Bangladesh National Herbarium, Dhaka authority, and the DACB accession number was 48087. The collected stem bark was washed with clean water, sun dried for seven to ten days and then kept in an electric oven for 72 h at 40 °C. After drying, the dried materials were ground into coarse powder with a grinding machine (FFC15, China), extracted by shaking with methanol (methyl alcohol) and sequentially fractionated with *n*-hexane, chloroform, and ethyl acetate (ester). The resultant fractions, such as the *n*-hexane fraction (NHF), chloroform fraction (CHF), ethyl acetate fraction (EAF) and aqueous fraction (AQF), were used for further investigation. The overall methodology flow diagram is shown in Fig. 1.

2.3. Evaluation of in vitro anti-inflammatory activity

The anti-inflammatory activities of crude methanolic extract (CME) and its fractions were assayed by the human red blood cell (HRBC) membrane stabilization method and inhibition of egg albumin denaturation assay.

2.3.1. Membrane stabilization method

The membrane-stabilizing activity was determined as described by Anosike et al., 2012 and G. Leelaprakash et al., 2011 [18,19]. Stabilization of HRBC by heat- or hypotonicity-induced membrane lysis was performed by the following two methods.

2.3.1.1. Hypotonicity-induced hemolysis of HRBC membranes. Blood samples were withdrawn from a healthy human volunteer who had not taken any NSAIDs for 14 days before the experiment and centrifuged at 700×*g* for 5 min, and the supernatant was removed. The packed blood corpuscles (cells) were washed with iso-saline, and a suspension (10%) was made. Isotonic solutions (in PBS) of CME and different fractions of 100, 200, 300, 400 and 500 μg/mL concentrations were separately mixed with 2 mL hyposaline solution (0.36%) and 0.5 mL HRBC suspension. The mixtures were incubated for 10 min at room temperature and centrifuged for 5 min at 2800 g, and the absorbance of the supernatant was measured at 540 nm using a spectrophotometer. The reference standard was acetyl salicylic acid (ASA) at concentrations of 100, 200, 300, 400, and 500 μg/mL. The HRBC membrane stabilization or protection percentage was calculated by the following formula (i):

$$\text{Inhibitionofhemolysis}(\%) = 100 \times \left(1 - \frac{OD2 - OD1}{OD3 - OD1}\right) \quad \text{(i)}$$

where OD_1 = test sample in isotonic solution, OD_2 = test sample hypotonic solution, and OD_3 = control sample in hypotonic solution.

2.3.1.2. Heat-induced hemolysis of the HRBC membrane. The assay mixture comprised 1 mL of test sample (CME/fractions/acetyl salicylic acid as standard) at 100, 200, 300, 400 and 500 μg/mL concentrations in isotonic PBS and 1 mL of 10% RBC suspension. The reaction mixtures were then incubated at 54 °C for 20 min in a water bath and centrifuged for 5 min at 2800 g, and the absorbance of the supernatant was measured using a spectrophotometer at 540 nm. The percent inhibition of hemolysis was calculated according to the following equation:

$$\text{Inhibitionofhemolysis}(\%) = 100 \times \left(1 - \frac{OD2 - OD1}{OD3 - OD1}\right) \quad \text{(ii)}$$

where OD_1 = unheated test sample, OD_2 = heated test sample, and OD_3 = heated control sample.

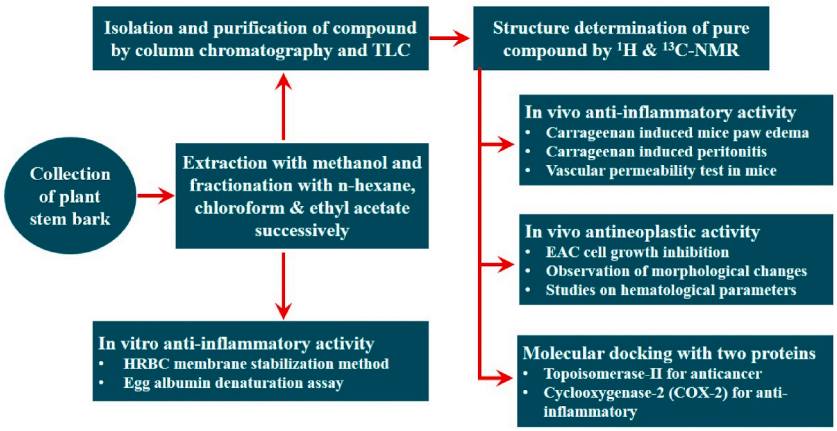

Fig. 1. Methodology flow diagram.

2.3.2. Egg albumin denaturation assay

To evaluate the inhibition of egg albumin denaturation, a reaction mixture of 5 mL consisting of 0.2 mL of egg albumin (from fresh hen's egg) and 2.8 mL of phosphate buffer saline (PBS, pH 6.4) including 2 mL of CME/fraction solutions of different concentrations (100, 200 and 400 μg/mL) in isotonic PBS was prepared. Distilled water with a similar volume was used as a control. The reaction mixtures were then incubated at 37 °C in an incubator for 15 min followed by heating at 70 °C for 5 min. The absorbance was measured after cooling by using a spectrophotometer at 660 nm. Acetyl salicylic acid (ASA) was used as a reference standard drug at concentrations of 100, 200 and 400 μg/mL and treated similarly for absorbance determination. The inhibition percentage of hemolysis was enumerated according to the equation [20].

$$\text{Inhibitionofhemolysis}(\%) = 100 \times \left(1 - \frac{OD2 - OD1}{OD3 - OD1}\right) \quad \text{(iii)}$$

where OD_1 = test sample in isotonic solution, OD_2 = test sample hypotonic solution, and OD_3 = control sample in hypotonic solution.

2.4. Compound isolation and characterization by chromatographic techniques

In the *in vitro* anti-inflammatory assay, CHF had more influential activity than the other fractions, and the TLC assay conjointly exhibited some distinct and outstanding spots. As a result, later bioactive compound isolation and purification was targeted at CHF. CHF was then subjected to column chromatography packed with 70–230 mesh silica gel. The solvent system was chloroform:methanol (3:1). A total of 262 fractions (test tubes with elute) were collected. Fractions 66 to 98 were combined due to similar spots on TLC under UV, iodine vapor and vanillin sulfuric acid spray reagents, and the solvent of the respective band was evaporated under reduced pressure to afford the compound (347.8 mg, $R_f = 0.4$) as colorless needle-like crystals. The compound was dissolved in methanol for analysis. The isolated compound structure was elucidated from ^{1}H- and ^{13}C-NMR spectra data and by comparison with reports in the literature [21]. The spectrum of the isolated pure compound was recorded on a Jeol-Ex at 400 MHz and 100 MHz and on FT NMR spectrometers, and methanol was the solvent.

2.5. Evaluation of the in vivo anti-inflammatory activity of the pure compound

2.5.1. Ethics of experimentation

Male Swiss albino mice of 21–28 days of age, weighing 25–30 g, were collected from the animal research branch of the Department of Pharmacy, Jahangirnagar University, Dhaka, Bangladesh. After the collection of mice, they were kept in standard and proper laboratory conditions and fed a commercially available pellet diet and normal clean water. The *in vivo* experiments were conducted based on the animal ethics guidelines of the Institute of Biological Sciences, University of Rajshahi, Bangladesh (Ethical Approval No: 124/320/IAMEBBC/IBSc, Date: 08 July 2019).

2.5.2. Acute toxicity study

The acute toxicity study of the isolated pure compound was carried out according to Chinedu et al., 2013 [22] with slight modifications to define the range of lethal doses as well as safe doses for the compound. To carry out the test, 18 Swiss albino male mice were used that were starved of food for 18 h but allowed access to water, and they were divided into 6 groups of 3 mice each and treated intraperitoneally with the isolated pure compound at various doses, such as 10, 25, 50, 100 and 200 mg/kg body weight. After the treatment, the mice were observed for dullness, nervousness, incoordination and/or mortality for 24 h. Based on the preliminary acute toxicity testing results, the doses of the isolated pure compound for further studies were concluded to be 25 and 50 mg/kg bodyweight of the mice.

2.5.3. Carrageenan induced hind paw edema in mice

In this study, 20 Swiss albino male mice were used, and they were classified into four groups. Each group contained five mice (N = 5). They (mice) were starved nightlong with free access to drinking water after the experiment. At the time of the experiment, baseline mouse paw volumes were recorded. Then, each group was intraperitoneally administered 0.9% normal saline, diclofenac-Na (50 mg/kg), and various doses of the pure compound (25, 50 mg/kg) as the control, reference, and test groups, respectively. After 60 min of administration of the sample, paw edema of mice was induced by subplantar administration of 1% carrageenan (0.1 mL) in normal saline into the right hind paw of the mice. After that, the paw volume increase was measured at 1, 2, 3, 4, 5 and 6 h post carrageenan administration. The mean hind paw swelling of the treated group mice was compared with that of the untreated control group mice. The inhibition of paw edema formation as a percentage was determined by the following formula [23]:

$$\%\ \text{Inhibition} = 100 \times \frac{(A - B)}{A} \quad \text{(iv)}$$

where A = carrageenan alone-treated group paw volume and B = tested group paw volume.

2.5.4. Carrageenan-induced peritonitis in mice

Peritonitis in mice was induced by the technique described in Gupta et al. [23] with slight modification. Twenty male Swiss albino mice (25–30 g) were randomly assigned into 4 groups, where group-1 was treated with vehicle (control), groups-2 and 3 with isolated

compound (25 and 50 mg/kg) and group-4 with diclofenac-Na (50 mg/kg). Treatments were given intraperitoneally. Carrageenan (0.25 mL, 1% in saline) was injected intraperitoneally 1 h later, and after 4 h, the animals were sacrificed with anesthesia, and the peritoneal cavity was washed with 3 mL of PBS containing 0.5 mL of 10% EDTA. A Neubauer chamber was used to determine the total WBC count, and microscopic counting was used to determine the differential cell count (Alves, 2009). The leukocyte migration inhibition percentage was calculated by this equation:

$$\text{Percentageinhibitionof WBCmigration} = 100 \times \left(1\text{-}\frac{T}{C}\right) \quad \text{(v)}$$

where T = WBC counts of the treated group and C = WBC counts of the control group.

2.5.5. Vascular permeability test in mice

This experiment is based on the IV injection of Evans blue (a dye) in a mouse model (test animal), where Evans blue binds with albumin, a simple protein. The activity of the isolated pure compound on acetic acid-induced mouse vascular permeability was evaluated by the method described by Zhao with some modifications [24]. Here, 20 Swiss albino male mice were subjected to four groups of 5 mice each used for the test, and group-1 was treated with vehicle (control), groups-2 and 3 with isolated compounds (25 and 50 mg/kg) and group-4 with diclofenac-Na (50 mg/kg). Prior to the experiment, the animals were starved for 10 h, and then varied doses of the compound and drug as stated above were administered intraperitoneally (IP). After 2 h, each animal was given a 0.2 mL IV injection of 1% Evans blue solution. Vascular permeability was induced half an hour afterwards by IP injection of 0.3 mL of 0.6% acetic acid (1 mL/100 g). After 20 min, the animals were sacrificed, and their peritoneum was washed with 5 mL of normal saline. The collected peritoneal fluid was centrifuged, the absorbance of the supernatant was measured using a spectrophotometer at 610 nm, and the percent inhibition of vascular permeability was enumerated by the equation stated below:

$$\%\ \text{Inhibition of vascular permeability} = [(A_0\text{-}A_1)\ /\ A_0] \times 100 \quad \text{(vi)}$$

where A_0 = absorbance of the control. A_1 = Absorbance of compound/reference standard.

2.5.6. Extraction of Evans blue from the mouse liver

After sacrificing the mice through cervical dislocation, the livers were collected and weighed. Then, the collected livers were washed with normal PBS and placed in 2 mL scientific specimen jars. Then, 500 μL of normal saline was added to each tissue sample (liver) jar. Then, all specimen jars were incubated at 55 °C for 24–48 h to extravasate Evans blue from the liver. The normal saline/Evans blue mixed solutions were centrifuged for 10 min at 1792 g to pellet any residual liver tissue fragments. Then, the supernatant absorbance was measured at 610 nm. Finally, the amount of extravasated Evans blue (per mg tissue) was determined from the Evans blue standard curve [25].

2.6. Evaluation of in vivo antineoplastic activity

2.6.1. Animal model

Swiss albino male mice aged 21–28 days and weighing 25–30 g were collected from the animal house of the Department of Pharmacy, Jahangirnagar University, Dhaka, Bangladesh. They were kept under standard laboratory conditions of temperature 22–28 °C and humidity 55% with 12 h day-night cycles, and their diet was standard dry pellets and clean water.

2.6.2. Tumor model of the experiment

The Ehrlich ascites carcinoma (transplantable tumor) used in this experiment was collected from the Department of Biochemistry and Molecular Biology, University of Rajshahi, Bangladesh. Here, for tumor aspiration, a 5 mL syringe fitted with a 20-gauge needle was used. Normal saline was used for dilution of freshly drawn fluid, and a hemocytometer was used for counting the number of tumor cells, which was adjusted to approximately 3×10^6 cells/mL. The viability of EAC cells was examined by a 0.4% trypan blue dye exclusion assay. For transplantation, the cell sample used showed above 90% viability. A 0.1 mL tumor suspension was intraperitoneally injected into each mouse. Throughout the transplantation process, strict aseptic conditions were maintained [26].

2.6.3. Collection of EAC cells

Ehrlich's ascites carcinoma (EAC) cells collected from donor Swiss albino male mice weighing 25–30 g were suspended in sterile isotonic saline. As described in the above experimental method, a fixed number of viable EAC cells (usually 1.5×10^6 cells/mL) were then implanted into the peritoneal cavity of each recipient mouse as a control. On the sixth day, the mice were sacrificed, and the intraperitoneal tumor (EAC) cells were harvested with normal saline.

2.6.4. Antineoplastic activity of the isolated compound

EAC is a rapidly growing experimental tumor with very aggressive behavior and resembles human tumors. In cancerous mice, the number of EAC cells and WBCs grow very rapidly, while RBC count and Hb content are reduced due to iron deficiency or hemolytic or myelopathic conditions. Anticancer agents return these altered parameters to normal values [27,28]. The antineoplastic activity (*in vivo*) of the isolated compound was examined by measuring the effect on tumor cell growth, hematological parameters of mice bearing EAC cells and morphological changes in EAC cells [29].

2.6.4.1. Studies on the growth inhibition of EAC cells. Four groups of Swiss albino male mice weighing 25–30 g were used to determine the EAC cell growth inhibition properties of the compound. Each group contained 6 mice. To assess the therapeutic evaluation of the sample, 1.6×10^6 tumor cells (EAC) were inoculated into each mouse group on day zero. Twenty-four hours after tumor inoculation, treatments were started and continued for five days. In brief, the mice in group 1 were considered untreated EAC controls, groups 2 and 3 received isolated compounds at 25 and 50 mg/kg/per day doses, respectively, and group 4 received the standard drug vincristine via intraperitoneal injection. On day six, each group of mice was sacrificed, and the total intraperitoneal tumor cells were harvested with normal saline (0.98%). First, the viable cells were identified with trypan blue and then counted with the help of a hemocytometer under an inverted microscope (XDS-1R, Optika, and Bergamo, Italy).

2.6.4.2. Studies on morphological changes in EAC cells. Normal EAC cells are approximately round and regular in shape. After treatment, apoptotic morphologic alterations, such as membrane and nuclear condensation or fragmentation, were observed. To examine the morphological appearances of tumor (EAC) cells, DAPI (4,6-diamidino-2-phenylindole) was used. The cells were collected from nontreated EAC-bearing mice and mice treated with isolated compounds (25 and 50 mg/kg/day) for 7 days and then stained with DAPI. Finally, the cells were observed under a fluorescence microscope, and images were taken. Both optical and fluorescent views were observed.

2.6.4.3. Studies on mouse hematological parameters. To evaluate the effects of the isolated compound on the hematological parameters of tumor-bearing mice, a comparison among five groups ($N = 6$) of mice was made on the 12th day after inoculation. EAC cells (0.1 mL of 1.6×10^6 cells/mice) were injected intraperitoneally into all the groups except the normal group (group-1) on day zero. Twenty-four hours after tumor inoculation, normal saline (5 mL/kg/mouse/day) was intraperitoneally administered to normal (group-1) and EAC control (group-2) mice for ten days. The isolated compounds at doses of 25 and 50 mg/kg/mouse/day were injected into group-3 and group-4, respectively, and group-5 received treatment with vincristine as a standard. On the 12th day after treatment, hematological parameters, including hemoglobin, RBCs and WBCs, were measured from blood collected from the tail vein of each mouse in each group, and hematological parameters were measured by following previously described methods with modifications [30].

2.6.4.4. Measurement of hemoglobin (Hb). The hemoglobin (Hb) content was measured using Shali's hemometer. Twenty microliters of noncoagulating blood was placed in a hemometer cuvette (tube) containing a small amount of N/10 HCl. Some distilled water was added and stirred continuously until a good color match was observed. The final reading of the solution in the cuvette was noted, and finally, the hemoglobin content (g/dL) was calculated from the cuvette reading.

2.6.4.5. Total WBC count. Exactly 10 μL of blood (noncoagulating) was drawn by a micropipette, diluted with 1 mL of WBC counting fluid and mixed gently and properly. The prepared mixture was observed using a hemocytometer, the number of WBCs was counted under a microscope, and the dilution factor was 100. Finally, the total WBC/mL was calculated.

2.6.4.6. Total count of RBCs. Exactly 10 μL of blood (noncoagulating) was drawn by a micropipette and diluted 1000 times with RBC counting fluid. Finally, similar to the WBC counting technique, total RBCs were counted with a hemocytometer.

2.7. Retrieval and preparation of receptor proteins and ligands

Two proteins, topoisomerase-II for anticancer activity and cyclooxygenase-2 (Cox-2) for anti-inflammatory activity, were selected for molecular docking with the isolated compound. The three-dimensional (3D) structures of these proteins were downloaded from the RCSB Protein Data Bank (PDB) in.pdb format (https://www.rcsb.org/; accessed on 22 June 2023). AutoDock Vina, Vina Wizard, and Open Babel of PyRx virtual screening software [31] were used for the docking studies. The docking output expressed in binding affinity/energy (kcal/mol) shows the interaction energy between the protein and the ligands/drug compounds. The water molecules and heteroatoms from the downloaded proteins were deleted, and polar hydrogen atoms were added using Biovia Discovery Studio software 2021 (v21.1.0.20,298). Then, each protein was loaded in PyRx software to convert the PDB structure of the prepared macromolecules to PDBQT format. The structures of trans-syringin were retrieved as an SDF file from the PubChem database (https://pubchem.ncbi.nlm.nih.gov) [32]. The file was converted to PDB format with the help of Open Babel software (http://openbabel.org) [33]. To carry out molecular docking, the ligand was optimized, energy minimization was performed, and the pdbqt file was constructed with the help of the Autodock tool (ADT). The ligand trans-syringin was imported into PyRx, and the open Babel energy was minimized and converted to PDBQT format. Then, Vina wizard was run, the ligand and proteins were selected, and the grid box was constructed specifying the X, Y and Z coordinates of the macromolecule. Protein–ligand interactions were visualized using Discovery Studio to further understand the amino acids and the kinds of bonds interacting in the binding sites.

2.8. Statistical analysis

All data are presented as the mean ± standard deviation (SD). Statistical analysis and calculation were performed with one-way ANOVA (analysis of variance) followed by Dunnett's 't' test using IBM-SPSS/20 and GraphPad Prism 8. $P < 0.05$ was recommended to indicate that the data were statistically significant.

3. Results

3.1. Evaluation of in vitro anti-inflammatory activity

3.1.1. HRBC membrane stabilization capacity

3.1.1.1. Heat-induced hemolysis of the HRBC membrane. The results (shown in Fig. 2) of the anti-inflammatory activity of CME and different fractions at various concentrations protected the human RBC membrane against heat-induced lysis, as shown by the high percentage inhibition of RBC membrane hemolysis. At a concentration of 300 μg/mL, CME, NHF, CHF, EAF, and AQF exhibited 33.17 ± 1.56%, 16.08 ± 0.98%, 50.75 ± 1.05%, 35.11 ± 0.70% and 22.31 ± 4.52% inhibition of HRBC hemolysis, respectively, compared with 61.54 ± 2.69% inhibition produced by the same concentration of standard acetyl salicylic acid (ASA). At 500 μg/mL (higher) concentration, CME, NHF, CHF, EAF, and AQF exhibited 51.29 ± 0.98%, 38.8 ± 1.06%, 73.91 ± 1.70%, 59.15 ± 0.98% and 40.98 ± 3.39% inhibition of HRBC hemolysis, respectively, compared with 84.34 ± 0.67% inhibition produced by the same concentration of standard ASA. The results obtained in this experiment indicated a greater response of CHF than EAF, CME, AQF, and NHF at all concentrations and lower than the standard.

3.1.1.2. Hypotonicity-induced hemolysis of HRBC membranes. The results (shown in Fig. 3) of the hypotonicity-induced hemolysis assay showed that CME and different fractions significantly inhibited lysis induced by vehicle. Hemolysis inhibition was dose dependent and increased with increasing concentrations of CME/fractions/standard acetyl salicylic acid. At the highest concentration (500 μg/mL), CME/fractions showed maximum percent inhibition of hemolysis. Among all the fractions, CHF and EAF showed the highest inhibition of hemolysis (75.92 ± 0.14% and 63.59 ± 3.54%, respectively) compared with the standard ASA, whose inhibition was 83.32% at the same concentration. The results obtained in this experiment indicated a higher response of CHF and EAF than CME, AQF and NHF at all concentrations.

3.1.2. Egg albumin denaturation assay

This assay showed that the inhibition of albumin (protein) denaturation by the test samples was concentration dependent throughout the range of 100–400 μg/mL, and acetyl salicylic acid was used as the standard drug at the same concentration. The inhibitory effect of CME and different fractions of the investigated plant is shown in Fig. 4. Hence, it may be said that the investigated CME of plant extract and its fractions may have moderate to potent anti-inflammatory activity.

3.2. Characterization of the isolated compound

Fig. 5(a and b) represents the ^{1}H-NMR (MeOD, 400 MHz) and ^{13}C-NMR (MeOD, 125 MHz) data of the isolated pure compound. The ^{1}H-NMR data of the isolated bioactive pure compound showed a typical singlet integrating two protons pointing at δ_H 6.75 ppm (H_5, H_9), representing the existence of a symmetric tetra-substituted aromatic ring and another singlet at δ_H 3.85 ppm (6H) attributable to an aromatic ring system with two methoxy groups. The observation of two characteristic doublets at δ_H 6.54 (1H, $J = 15.9$ Hz) and δ_H 6.34 (overlapped signal, 1H, $J = 15.9$ Hz) represented the existence of a trans di-substituted double bond directly linked to a methylene group with δ_H 4.23 (overlapped, d, 5.5). The ^{13}C-NMR spectrum showed the famous peak of anomeric carbon C_1' at δ_C 105.4 ppm and five peaks appearing between δ_C 62.6 ppm and δ_C 78.3 ppm attributable to C_2', C_3', C_4' and C_5' of a glycopyranose moiety, indicating that the isolated pure compound is an aromatic glycoside derivative (Table 1).

On the basis of the ^{1}H-NMR and ^{13}C-NMR spectra and comparison with syringin (known) derivatives (Fig. 6) [34], the isolated pure compound (Sz-01) was identified as hydroxypropenyl dimethoxyphenyl-β-D-glucoside (trans-syringin).

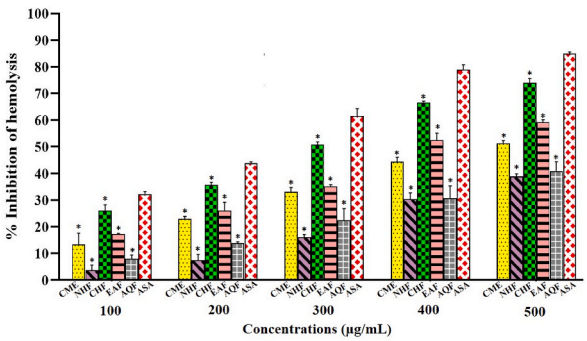

Fig. 2. Percentage inhibition of heat-induced hemolysis of the HRBC membrane by CME and its fractions.

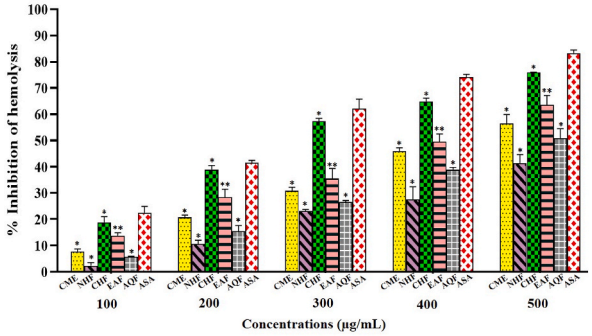

Fig. 3. Percentage inhibition of hypotonicity-induced hemolysis of the HRBC membrane by crude methanolic extract and fractions.

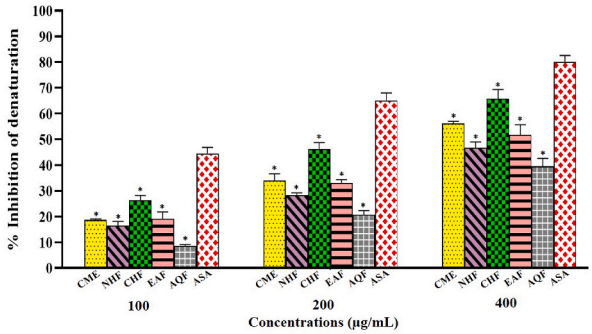

Fig. 4. Percentage inhibition of egg albumin denaturation by CME and its fractions.

3.3. Evaluation of the in vivo anti-inflammatory activity of the pure compound

3.3.1. Evaluation of carrageenan-induced mouse hind paw edema

In all the tested groups of male Swiss albino mice, an increase in hind paw edema was created by administering carrageenan in a time-dependent manner, as shown in Table 2.

After treatment with compound and standard diclofenac-Na, paw edema was decreased at 6 h post carrageenan administration in a dose-dependent manner. It was observed that a 50 mg/kg body weight concentration showed maximum anti-inflammatory activity (reduction in paw edema). An illustration of this effect is shown in Fig. 11. The inhibition obtained with the isolated pure bioactive compound (trans-syringin) was 60.46% and 62.9% for standard diclofenac-Na.

3.3.2. Evaluation of carrageenan-induced peritonitis in mice

Carrageenan is responsible for inflammation, and through the induction of peritonitis by carrageenan, it was observed that the white blood cell population was significantly increased in the inflammatory exudates and that the WBC count was higher in the carrageenan-treated group of mice than in the compound-treated group of mice. Intraperitoneal treatment was carried out with the isolated bioactive pure compound (trans-syringin) and standard diclofenac-Na. A significant decrease in WBC count was observed in the peritoneal fluid: 36.35 ± 1.38% inhibition for 25 mg/kg body weight, 61.89 ± 1.76% inhibition for 50 mg/kg body weight for trans-syringin and 71.52 ± 0.33% inhibition for 50 mg/kg body weight for diclofenac-Na, as shown in Fig. 7.

3.3.3. Effect of the isolated compound (trans-syringin) on acetic acid-induced vascular permeability

Vascular permeability is increased during inflammation or any other disease condition and is expressed by the amount of Evans blue that is extruded into the peritoneal cavity. The absorbance value of the acetic acid-control group markedly increased after the administration of acetic acid to the mice, and treatment with the isolated compound (trans-syringin) (50 mg/kg) significantly produced an inhibitory effect of 70.24 ± 1.18% compared with 80.02 ± 1.39% inhibition produced by standard diclofenac-Na at the same dose (Fig. 8). These data showed that the isolated pure compound (trans-syringin) inhibited vascular permeability induced by acetic acid.

3.3.4. Quantification of Evans blue extravasation from liver tissue

The absorbance value is used to measure the difference in blood vessel permeability by spectrophotometrically quantifying Evans blue, which is calculated per gram of liver tissue. Various concentrations of isolated compound (trans-syringin) and standard show various responses to permeability inducer signals and thus show various dye accumulation. At a concentration of 50 mg/kg body

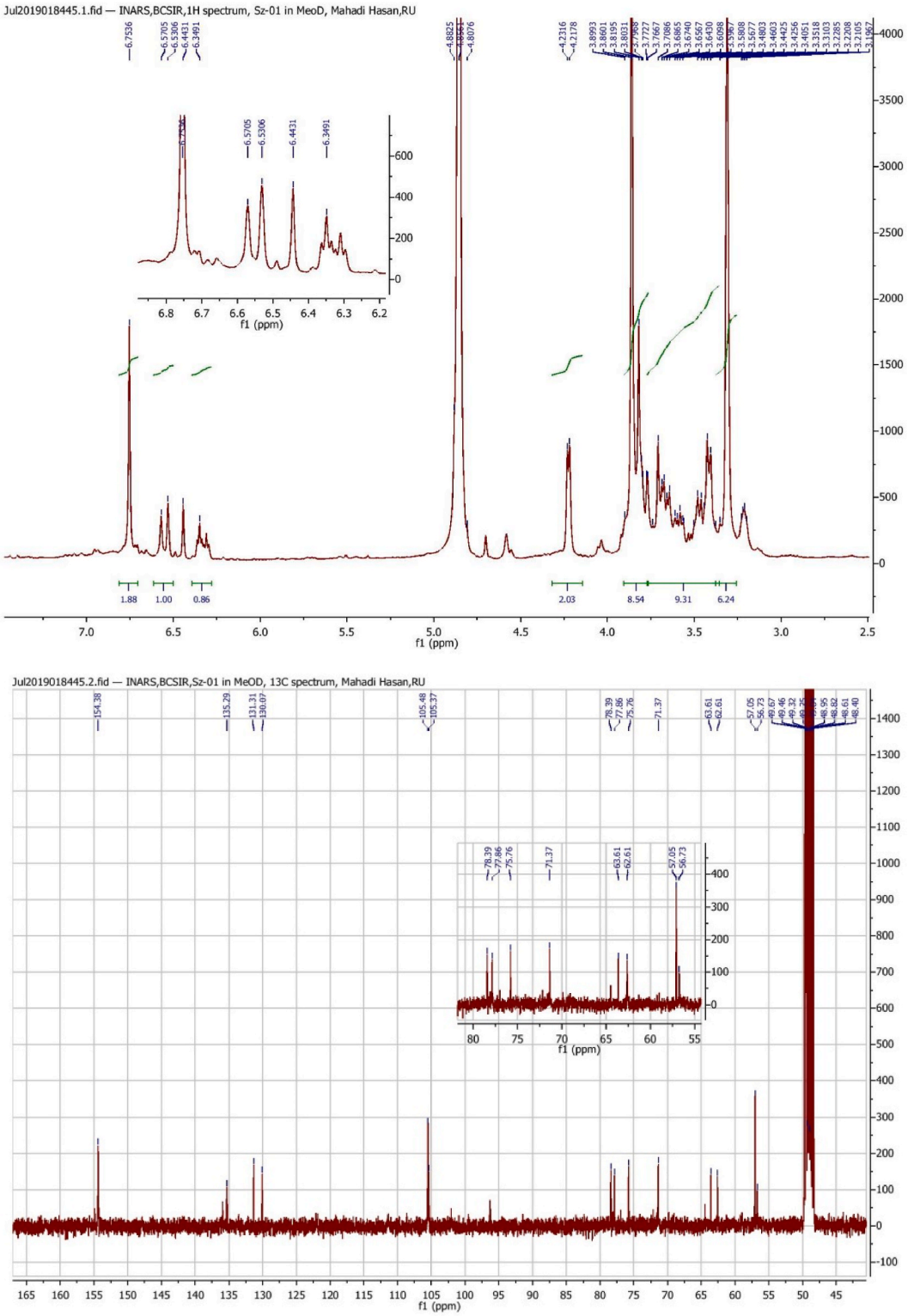

Fig. 5. NMR spectra of trans-syringin (Sz-01); a) ^{1}H-NMR and b) ^{13}C-NMR.

Table 1
^{1}H (400 MHz) and ^{13}C-NMR (125 MHz) spectral data of TS.

Position	δ_C	δ_H(J in Hz)
1	63.6	4.3 (Overlapped, d, 5.5)
2	13.07	6.34 (Overlapped, dd.15.9, 5.5)
3	131.3	6.54 (d, 15.9)
4	135.2	–
5,9	105.3	6.75 (s)
6,8	154.3	–
7	–	–
1′	105.4	4.8 (Overlapped)
2′	71.3–78.3	3.0–3.8 (m)
3′	71.3–78.3	3.0–3.8 (m)
4′	71.3–78.3	3.0–3.8 (m)
5′	71.3–78.3	3.0–3.8 (m)
6′	62.6	3.64 (dd), 3.77 (dd)
10,11 (-OCH_3)	57.05	3.85 (6H,s)

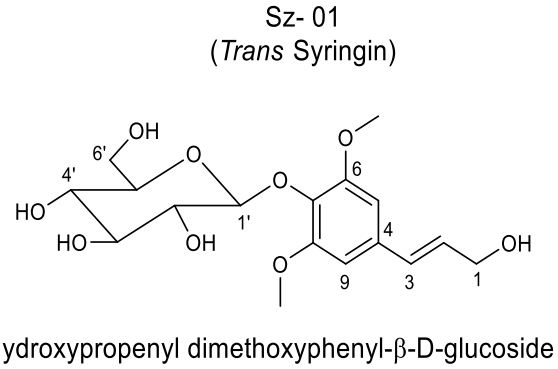

Fig. 6. Structure of the isolated compound trans-syringin.

Table 2
Inhibitory effect of trans-syringin and diclofenac-Na on carrageenan-induced paw edema in mice.

Treatment	% Inhibition of edema					
	1 h	2 h	3 h	4 h	5 h	6 h
Control	–	–	–	–	–	–
Trans-Syringin (25 mg/kg)	39.86 ± 0.03 **	39.75 ± 0.11**	42.69 ± 0.07*	43.33 ± 0.48**	50.36 ± 0.32*	53.81 ± 0.13**
Trans-Syringin (50 mg/kg)	45.63 ± 0.18 *	47.63 ± 0.97*	51.08 ± 0.08	53.33 ± 0.72*	56.18 ± 0.34**	60.26 ± 0.98
Diclofenac-Na (50 mg/kg)	54.19 ± 0.01	55.36 ± 0.22	60.64 ± 0.19	61.74 ± 0.47	62 ± 0.04	62.9 ± 0.18

*$p < 0.05$, **$p < 0.01$ compared to the reference standard drug-treated group. Data are expressed as the mean ± SD. Analysis of variance followed by Dunnett's post hoc test (IBM-SPSS/20).

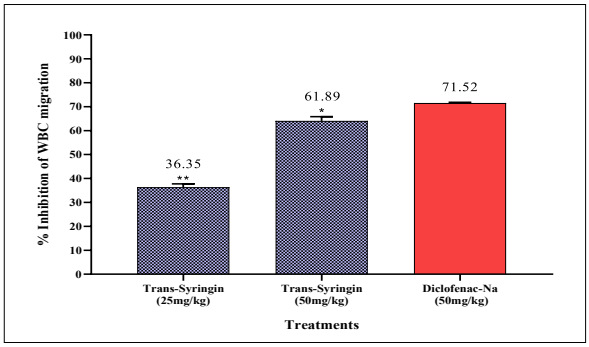

Fig. 7. Percentage inhibition of WBC migration by trans-syringin and diclofenac-Na.

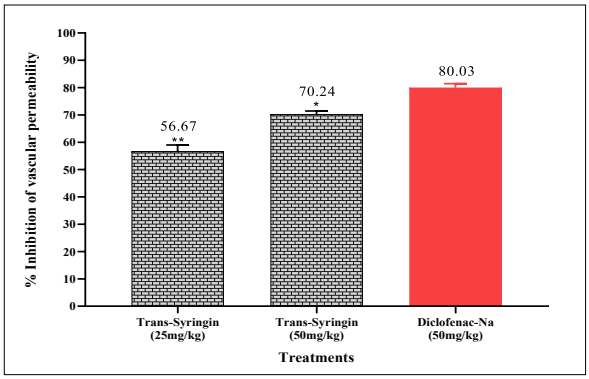

Fig. 8. Inhibitory effect of trans-syringin on vascular permeability compared with that of diclofenac-Na.

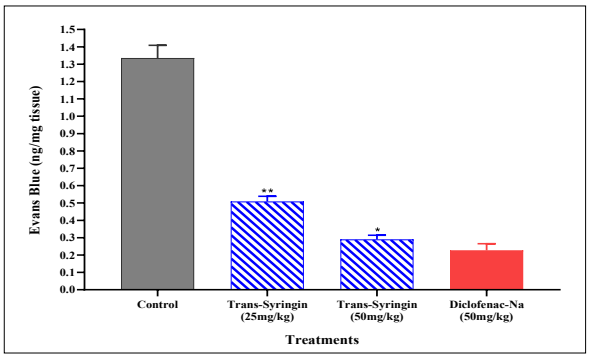

Fig. 9. Quantitation of Evans blue extravasation from liver tissues in different groups.

weight, the compound exhibited the lowest amount of Evans blue, with a value of 0.289 ± 0.02 ng/mg liver tissue, compared with 0.227 ± 0.03 ng/mg liver tissue produced by standard diclofenac-Na at 50 mg/kg (Fig. 9).

3.4. Evaluation of in vivo antineoplastic activity

3.4.1. Studies on EAC cell growth inhibition

The anticancer effect of the isolated compound (trans-syringin) on EAC cells was assessed *in vivo* in terms of percent (%) inhibition of EAC cell growth after intraperitoneal transplantation, and the average cell count of the untreated control group was (6.337 ± 0.48) x 10^7 cells/mL/mice. Treatment with various concentrations of the isolated compound showed a significant reduction in cancer cell growth (Table 3).

At doses of 25 and 50 mg/kg of the compound, the growth inhibition of EAC cells was 45.26% and 68.31%, respectively, compared with the mice in the EAC control group ($p < 0.05$), whereas the standard drug vincristine (6.25 mg/kg) showed 73.26 ± 3.41% inhibition.

3.4.2. Examination of morphological changes in EAC cells

After continuous treatment for five days, cancer cells were collected from mice in the control and compound (trans-syringin)-treated groups, examined by DAPI (4′,6-diamidino-2-phenylindole) staining and viewed under fluorescence and optical microscopy. The microscopic view showed that the compound-treated EAC cell nuclei and membrane were fragmented and condensed, as shown in

Table 3
Effect of TS and VCR on Ehrlich ascites carcinoma (EAC) cell growth.

Group no.	Treatment	Viable EAC cells on day 6 after inoculation (×10^7 cells/mL)	% cell growth inhibition
1	EAC cell	6.337 ± 0.48	–
2	EAC + Trans-Syringin (25 mg/kg)	3.469 ± 0.16*	45.26 ± 2.24*
3	EAC + Trans-Syringin (50 mg/kg)	2.013 ± 0.24*	68.31 ± 3.26*
4	EAC + Vincristine (6.25 mg/kg)	2.015 ± 0.18*	73.26 ± 3.41*

*$p < 0.05$: Significant difference compared to the EAC control group. Data are expressed as the mean ± SD for six animals in each group. Analysis of variance followed by Dunnett's post hoc test (IBM-SPSS/20).

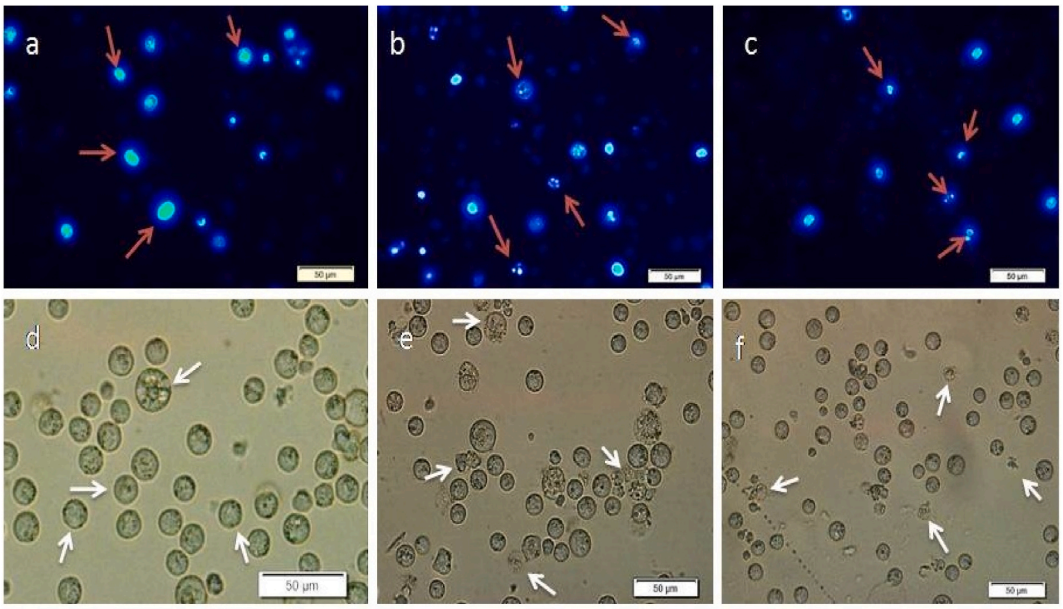

Fig. 10. (a, b & c) Fluorescence and (d, e & f) optical microscopic observation of EAC cells for control mice and mice treated with trans-syringin. (a, b & c) Fluorescence and (d, e & f) optical microscopic views of EAC cells from control mice and treated mice. (a) Fluorescence microscopic view of control mouse EAC cells, (b) fluorescence microscopic view of trans-syringin (25 mg/kg)-treated mouse EAC cells and (c) fluorescence microscopic view of trans-syringin (50 mg/kg)-treated mouse EAC cells. (d) Optical microscopic view of control mouse EAC cells, (e) optical microscopic view of trans-syringin (25 mg/kg)-treated mouse EAC cells and (f) optical microscopic view of trans-syringin (50 mg/kg)-treated mouse EAC cells. Control groups showed normal cells with round-shaped nuclei and are indicated by red and white arrows in (a) and (d), whereas the mice treated with pure compound showed condensed nuclei and fragmentation of cells (apoptotic characteristics), as shown in (b) and (e), (c) and (f), indicated by red and white arrows for trans-syringin (25 mg/kg) and trans-syringin (50 mg/kg), respectively.

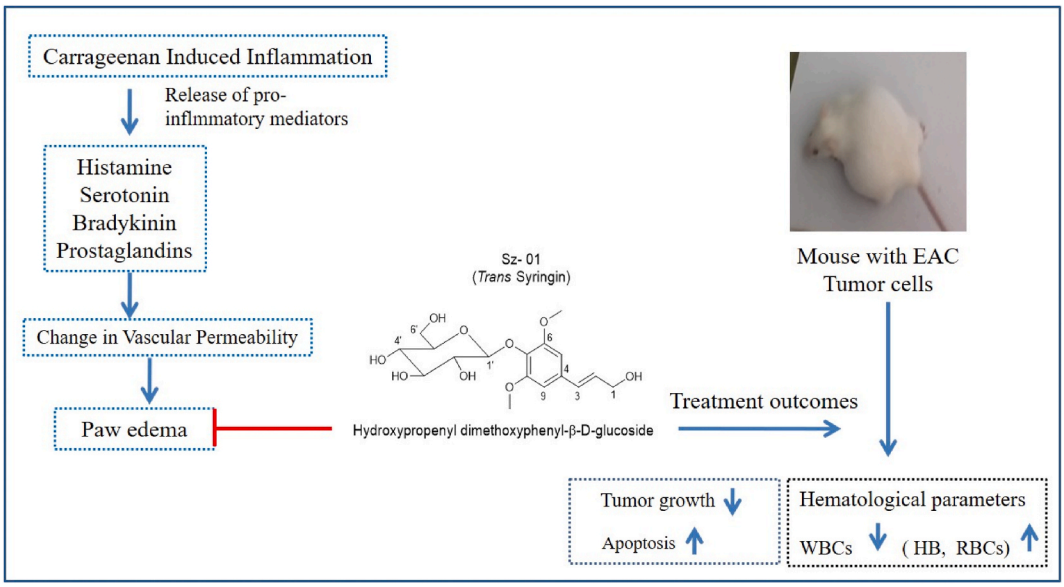

Fig. 11. An illustration of the anti-inflammatory and antineoplastic activities of pure compounds isolated from the EAF of *M. champaca.*

Fig. 10(a–f) and indicated by arrows. These findings showed that the isolated compound treatment could produce apoptosis in tumor (EAC) cells.

3.4.3. Studies on hematological parameters of mice

The hematological parameters of mice, such as red blood cell (RBC), white blood cell (WBC) and hemoglobin (Hb) content, of the

normal, untreated, and treated groups were examined. The untreated group (EAC + vehicle) showed significant ($P < 0.05$) changes in hematological parameters on day 12 compared to the normal group. In the untreated group, the hemoglobin content and total RBC count were found to decrease with an increase in the total WBC count; on the other hand, treatment with the isolated compound (trans-syringin) at 25 and 50 mg/kg returned the altered hematological parameters to normal values, which were comparable to those of standard vincristine (6.25 mg/kg). The overall data are furnished in Table 4, and an illustration of the antineoplastic activities is shown in Fig. 11.

3.5. Molecular docking analysis

The results of the molecular docking analysis are shown in Figs. 12 and 13 and are represented in the form of minimum binding energy values (Table 5).

Our results showed that trans-syringin and standard diclofenac sodium interacted with some amino acids of the cox-2 protein with binding affinities of -8.2 and -7.6 kcal/mol, respectively (Fig. 13a–d). Since the higher negative docking score represented a high binding affinity between the receptor and ligand molecules, showing the higher efficiency of bioactive compounds, the binding capacity of trans-syringin into the cox-2 binding site is greater than that of standard diclofenac sodium.

For the topoisomerase II target protein, trans-syringin interacted with a binding affinity of −6.4 kcal/mol with four conventional H-bonds with different amino acids in this complex (Fig. 12c and d). The standard drug vincristine showed a binding affinity of −7.3 kcal/mol, showing a conventional H-bond with the TrpA:78 amino acid (Fig. 12a and b).

4. Discussion

Medicinal plants are being vastly investigated to combat cancer and inflammatory damage because of growing concerns with acute and chronic diseases due to cellular inflammation and carcinogens and the insufficiency of existing therapies to tackle such diseases [35]. The capacity of the plant extracts has been tested with extracts from different plant parts as well as compounds isolated from such extracts to identify potential lead compounds for drug discovery. The major focus of our study was to investigate the extracts from stem bark of *M. champaca* in protecting cell and cellular components against damage by inflammation as well as to prevent neoplasms that can result from damage to genetic materials of the cell. At the same time, identification of the active compound responsible mainly for such activity was also important to facilitate further research for drug development because other parts of the plant have been investigated against several diseases by researchers with significant findings [36] along with traditional uses.

Initial experiments with the crude methanolic extracts and fractions evaluated the *in vitro* anti-inflammatory activity of the stem bark and showed a higher response by CHF and EAF along with moderate activity by CME in protecting human RBCs from membrane hemolysis and egg albumin from denaturation. This result was very significant because *in vitro* protection of human red blood cells and protein has been extensively used as a method for evaluating anti-inflammatory activity by most of the research [29]. Therefore, the most active part (CHF) was selected for further detailed investigation of phytochemical contents and their specific effects in the *in vivo* model.

Previous phytochemical studies by several researchers as well as some preliminary screening in the present research showed the presence of natural compounds, including glycosides, alkaloids, volatile oils, phenolic compounds such as flavonoids, leucoanthocyanidins, *p*-hydroxybenzoic acid, syringic acid, etc. [37], which were assumed to be responsible for the biological activity of the plant extract. The current investigation showed the presence of a glycosidic compound named hydroxypropenyl dimethoxyphenyl-β-D-glucoside (trans-syringin) as a major bioactive compound, which justifies previous assumptions behind the study.

The evaluation of the isolated compound (trans-syringin) for its capacity to prevent inflammation of cellular components and associated diseases such as cancer also showed its potential for investigation because of the significant dose-dependent inhibition of several symptoms and parameters of inflammation and cancer by an *in vivo* method, and the findings were similar to other studies carried out on the plant family [38,39]. In the *in vivo* evaluation, the compound showed dose-dependent inhibition of carrageenan-induced symptoms of inflammation, such as the formation of hind paw edema, peritonitis and vascular permeability of plasma, which are well-known consequences of cellular inflammation [40]. Such an *in vivo* effect again justifies the capability of the compound to combat inflammation in cells, and the results are significant compared to other potential research findings where similar dose-dependent activities were reported [41,42].

Investigation of the isolated compound for preventing uncontrolled cell growth in neoplasms was carried out in an EAC cell model, and the findings showed considerable activity in inhibiting cell growth as well as improving the hematological parameters toward normal values, which suggests the potential of the compound to prevent neoplasms or cancer because not only uncontrolled cell growth but also a decrease in RBC or hemoglobin content as well as increased WBC content is the major pathogenesis of neoplasms [6]. Several glycosides, including cardiac glycosides such as digoxin and digitoxin, have been reported to exert activity against neoplasms and are one of the major plant products under research consideration for chronic diseases along with their cardioprotective activity [43]. Therefore, the presence of a glycosidic compound (trans-syringin) in the extract of *M. champaca* bark also indicates the potential of the plant part as a research candidate to combat neoplasms, and the findings of the present research proved such potential. In our *in vitro* or *in vivo* analysis of the anti-inflammatory and antineoplastic activity of EAC/pure compound showed some good results.

In this study, for the first time, trans-syringin from this plant was docked with cyclooxygenase-2 and topoisomerase II enzymes to determine whether this compound can bind to the active site of these enzymes and inhibit their activity. This docking provides supportive evidence that verifies the anti-inflammatory and antineoplastic properties of this compound, as confirmed through *in vitro*/*in vivo* experimentation conducted within the framework of this research. Molecular docking is a technique used to discover novel

Table 4
Effect of trans-syringin and vincristine on the blood parameters of tumor-bearing and normal Swiss albino mice.

Group no.	Treatment	Hgb (g/dL)	RBC ($\times 10^9$ cells/mL)	WBC ($\times 10^6$ cells/mL)
1	Normal	15.46 ± 0.78	6.63 ± 0.23	9.61 ± 0.89
2	EAC + Vehicle	8.92 ± 0.50*	1.92 ± 0.41*	60.64 ± 3.57*
3	EAC + Trans-Syringin (25 mg/kg)	11.68 ± 1.19#	2.95 ± 0.19 #	28.23 ± 2.86 #
4	EAC + Trans-Syringin (50 mg/kg)	13.82 ± 1.15#	4.87 ± 0.54 #	15.48 ± 2.70 #
5	EAC + Vincristine (6.25 mg/kg)	12.32 ± 1.18#	4.12 ± 0.22 #	14.16 ± 1.97 #

*$p < 0.05$ against the normal group and #$p < 0.05$ against the EAC control group followed by Dunnett's t post hoc test (IBM-SPSS/20). Data are expressed as the mean ± SD for six animals in each group.

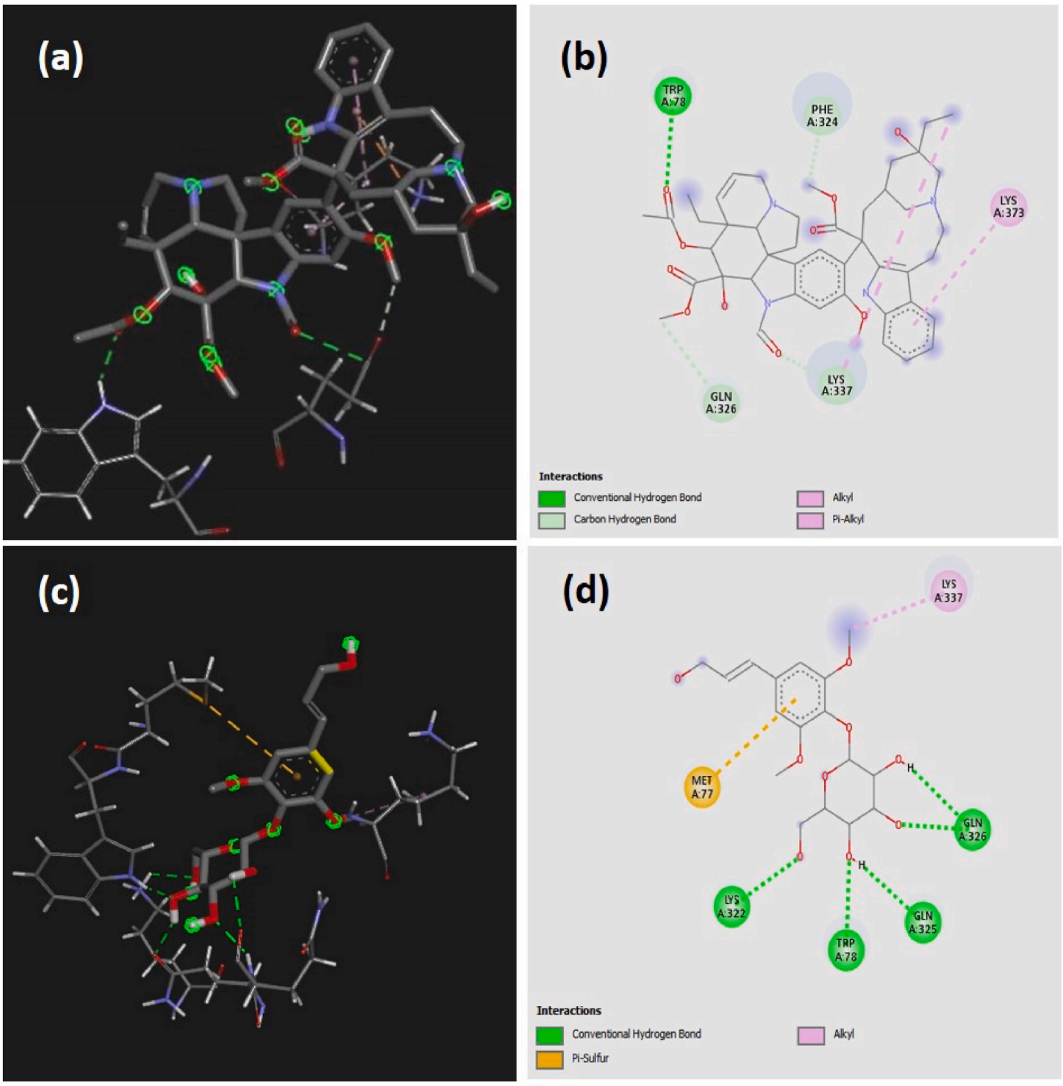

Fig. 12. 3D view (a) and 2D interaction of the vincristine-topoisomerase II complex and 3D view (c) and 2D interaction (d) of the trans-syringin-topoisomerase II complex at the binding site.

ligands for protein structure and plays an important role in structure-based drug design [44]. Topoisomerase II was targeted here, as it is a nuclear enzyme that changes the conformation of DNA and is involved in the separation of chromosomes and, therefore, is essential for cell division. All nucleated human cells and tumor cells contain topoisomerases, and the activity of this enzyme is essential for cell division because tumor cells divide in an uncontrolled manner. Various studies have proven that topoisomerase inhibitors are selectively toxic to tumor cells compared to normal cells and have proven their potential anticancer activity [45,46]. Loss of this enzyme's ability to rejoin DNA strands results in DNA damage and eventually apoptosis or cell death [47]. The isolated compound

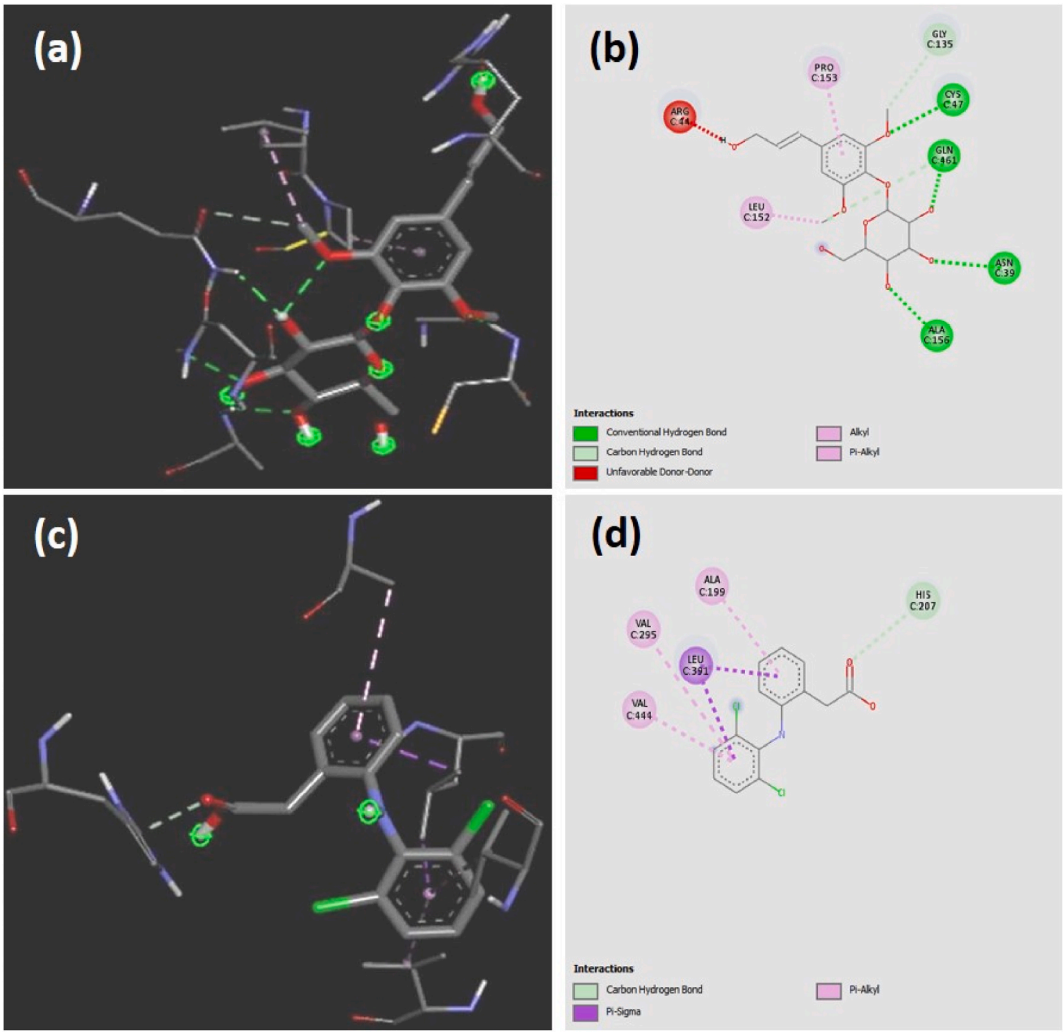

Fig. 13. a) 3D interaction diagram b) 2D interaction diagram of the transsyriginin-Cox2 complex and c) 3D interaction diagram d) 2D interaction diagram of the diclofenac-Cox2 complex at the binding site.

Table 5
Molecular docking score for the isolated compound with topoisomerase II and Cox-2 receptor proteins.

Ligand	Protein	Binding affinity (kcal/mol)	Interacting Amino Acids
Vincristine	Topoisomerase II	−7.3	TrpA:78, PheA:324 and GlnA:326
Trans-Syringin		−6.4	LysA:322, TrpA:78, GlnA:325
Diclofenac	Cox-2	−7.6	AlaC:199, ValC:295 and LeuC:391
Trans-Syringin		−8.2	CysC:47, GlnC:461, AsnC:39 and AlaC:156

trans-syringin interacted with LysA:322, TrpA:78, and GlnA:325 amino acid residues of the active pocket of topoisomerase-II with a Pi–sulfur interaction in the complex (Fig. 12c and d). The standard drug vincristine interacted with topoisomerase-II by binding to TrpA:78, PheA:324 and GlnA:326 amino acids; a pi-alkyl interaction was also observed with amino acid LysA:337 of its binding pocket (Fig. 12a and b). Inhibiting topoisomerase II can lead to DNA damage and cell death in cancer cells. This is a mechanism used by several chemotherapeutic drugs [48,49]. Trans-syringin exhibits a high affinity for topoisomerase II, indicating its potential to effectively inhibit the activity of this enzyme. This inhibition can disrupt tumor growth and promote cell death within cancerous tissues, thus positioning trans-syringin as a promising candidate for antineoplastic therapy.

On the other hand, cyclooxygenase-2 (Cox-2) is a crucial enzyme for catalyzing the synthesis of prostaglandins and is targeted for the treatment of inflammation. Docking of trans-syringin with Cox-2 revealed interactions with some amino acids having conventional H-bonds with CysC:47, GlnC:461, AsnC:39 and AlaC:156 amino acids in the complex (Fig. 13a and b). The standard diclofenac sodium (binding affinity of −7.6 kcal/mol) revealed interactions with AlaC:199, ValC:295 and LeuC:391 amino acids at the binding site of Cox-

2 (Fig. 13c and d), and a Pi–sigma (LeuC:391) was also observed in the complex. The Pi–sigma interactions (i.e., Pi–alkyl and Pi–sulfur) help to intercalate the drug in the binding pocket of the receptor, as they are largely involved in charge transfer. Moreover, the data obtained from the docking study align seamlessly with prior research findings on the polyphenolic compound quercetin, which interacts with the Cox-2 protein via several key amino acid residues, such as Cys 47 and Gln 461, and quercetin could be considered a selective Cox-2 inhibitor [50]. Similarly, our research extends this understanding by illustrating that trans-syringin also engages in interactions with Cox-2, forming hydrogen bonds with CysC:47 and GlnC:461.

This finding gains significant importance considering the central role played by the Cox-2 enzyme in the synthesis of inflammation-inducing prostaglandins. The binding of trans-syringin to Cox-2 implies its potential as an effective inhibitor of Cox-2 activity. Consequently, the inhibition of this enzyme can lead to a significant reduction in the production of inflammation-inducing prostaglandins, ultimately leading to the attenuation of the inflammatory response. Our findings not only corroborate the existing knowledge on Cox-2 inhibition by polyphenolic compounds but also shed light on the therapeutic potential of trans-syringin as a natural agent for mitigating inflammation through targeted interactions with Cox-2. This insight may pave the way for the development of novel anti-inflammatory treatments that harness the bioactive properties of trans-syringin. The docking analysis reveals how trans-syringin interacts with the active site of Cox-2 and topoisomerase-II, effectively inhibiting its enzymatic function. Since chronic inflammation is linked to the development and progression of various diseases, including cancer [51], this inhibition is critical in dampening the cascade of inflammatory events, which can contribute to the prevention and treatment of both inflammatory conditions and cancer, supporting its anticancer potential.

5. Conclusion

Our present investigation has shown that the stem bark extract and its different fractions from *M. champaca* exhibited *in vitro* anti-inflammatory activity against cellular inflammation, but the chloroform fraction (CHF) was the most predominant fraction to exhibit such activity. Further investigation of the CHF resulted in the isolation of a pure compound, which was defined as hydroxypropenyl dimethoxyphenyl-β-D-glucoside (trans-syringin). The compound showed potent *in vivo* anti-inflammatory and antineoplastic activity and promising binding affinity toward the two target proteins in molecular docking studies. The docking analysis not only validates the anti-inflammatory and antineoplastic properties of trans-syringin but also sheds light on the molecular mechanisms underlying its therapeutic effects. This information is invaluable for advancing our understanding of natural compounds such as trans-syringin and exploring their potential applications in the development of novel anti-inflammatory and anticancer treatments. Further investigations to analyze its bioactivity and clinical trials are necessary for the discovery of new drug formulations.

Funding and acknowledgment

The authors would like to extend their sincere appreciation to the Researchers Supporting Project Number (RSP2023R301), King Saud University, Riyadh, Saudi Arabia. The authors acknowledge the support of the Department of Pharmacy, University of Rajshahi, for providing the experimental facilities and equipment and the Department of Biochemistry and Molecular Biology, University of Rajshahi, for providing the EAC cells.

Data availability

Further data used to support the findings will be available from the corresponding author upon request.

CRediT authorship contribution statement

Md. Mahadi Hasan: Investigation. **Md. Ekramul Islam:** Writing - original draft. **Md. Sanowar Hossain:** Writing - review & editing. **Masuma Akter:** Formal analysis. **Md. Aziz Abdur Rahman:** Formal analysis. **Mohsin Kazi:** Writing - review & editing. **Shahzeb Khan:** Visualization. **Mst. Shahnaj Parvin:** Project administration.

Declaration of competing interest

The authors declare the following financial interests/personal relationships which may be considered as potential competing interests:

Mst. Shahnaj Parvin reports administrative support was provided by University of Rajshahi. Mst. Shahnaj Parvin reports a relationship with University of Rajshahi that includes: employment. Mst. Shahnaj Parvin has patent pending to Not applicable. Not applicable If there are other authors, they declare that they have no known competing financial interests or personal relationships that could have appeared to influence the work reported in this paper.

References

[1] L. Chen, et al., Inflammatory responses and inflammation-associated diseases in organs, Oncotarget 9 (6) (2018) 7204–7218.
[2] D.H. Tsai, et al., Effects of short- and long-term exposures to particulate matter on inflammatory marker levels in the general population, Environ. Sci. Pollut. Res. Int. 26 (19) (2019) 19697–19704.

[3] R.X. Wang, et al., The role of chronic inflammation in various diseases and anti-inflammatory therapies containing natural products, ChemMedChem 16 (10) (2021) 1576–1592.
[4] M.A. Rane, et al., Benefits and risks of nonsteroidal anti-inflammatory drugs: methodologic limitations lead to clinical uncertainties, Ther Innov Regul Sci 53 (4) (2019) 502–505.
[5] P. Chaiya, et al., In vitro anti-inflammatory activity using thermally inhibiting protein denaturation of egg albumin and antimicrobial activities of some organic solvents, Mater. Today: Proc. 65 (2022) 2290–2295.
[6] John Elflein, Predicted Number of Cancer Deaths Worldwide from 2020 to 2040, 2022. Statista.
[7] E.R. Mardis, R.K. Wilson, Cancer genome sequencing: a review, Hum. Mol. Genet. (R2) (2009) 18. R163-8.
[8] S.K. Bardaweel, et al., Reactive oxygen species: the dual role in physiological and pathological conditions of the human body, Eurasian J. Med. 50 (3) (2018) 193–201.
[9] L.L. Bennett, S. Rojas, T. Seefeldt, Role of antioxidants in the prevention of cancer, J. Exp. Clin. Med. 4 (4) (2012) 215–222.
[10] H. Maeda, M. Khatami, Analyses of repeated failures in cancer therapy for solid tumors: poor tumor-selective drug delivery, low therapeutic efficacy and unsustainable costs, Clin. Transl. Med. 7 (1) (2018) 11.
[11] M.S. Hossain, et al., Studies on in vitro antioxidant activity of methanolic extract and fractions of Ficus Hispida Lin. Fruits, J. Sci. Res. 8 (3) (2016) 371–380.
[12] S. Hossain, et al., An overview of the evidence and mechanism of drug-Herb interactions between propolis and pharmaceutical drugs, Front. Pharmacol. 13 (2022) 876183.
[13] G.M. Cragg, D.J. Newman, Natural products: a continuing source of novel drug leads, Biochim. Biophys. Acta 1830 (6) (2013) 3670–3695.
[14] S. Ali, et al., Biocompatible synthesis of magnesium oxide nanoparticles with effective antioxidant, antibacterial, and anti-inflammatory activities using Magnolia champaca extract, Biomass Convers. Biorefinery. 18 (2023) 1–12.
[15] F. Saqib, et al., Pharmacological basis for the medicinal use of Michelia champaca in gut, airways and cardiovascular disorders, Asian Pac. J. Trop. Med. 11 (2018) 292–296.
[16] M. Hasan, et al., Evaluation of antioxidant and antibacterial properties of magnolia champaca L (Magnoliaceae) stem bark extract, Bangladesh Pharmaceut. J. 23 (2020) 96–102.
[17] M.A. Loza-Mejía, J.R. Salazar, J.F. Sánchez-Tejeda, In silico studies on compounds derived from Calceolaria: phenylethanoid glycosides as potential multitarget inhibitors for the development of pesticides, Biomolecules (4) (2018) 8.
[18] C.A. Anosike, O. Obidoa, L.U. Ezeanyika, Membrane stabilization as a mechanism of the anti-inflammatory activity of methanol extract of garden egg (Solanum aethiopicum), Daru 20 (1) (2012) 76.
[19] G. Leelaprakash, S. Dass, Invitro Anti-Inflammatory Activity of Methanol Extract of Enicostemma Axillare, Int. J. Drug Dev. Res. 3 (3) (2011) 189–196.
[20] S. Chandra, et al., Evaluation of in vitro anti-inflammatory activity of coffee against the denaturation of protein, Asian Pac. J. Trop. Biomed. 2 (1, Supplement) (2012) S178–S180.
[21] Y. Zhang, et al., Purification and characterization of flavonoids from the leaves of Zanthoxylum bungeanum and correlation between their structure and antioxidant activity, PLoS One 9 (8) (2014), e105725.
[22] E. Chinedu, D. Arome, F.S. Ameh, A new method for determining acute toxicity in animal models, Toxicol. Int. 20 (3) (2013) 224–226.
[23] M. Gupta, et al., Antiinflammatory evaluation of leaves of Plumeria acuminata, BMC Compl. Alternative Med. 6 (2006) 36.
[24] Z. Zhao, et al., Anti-inflammatory effects of novel sinomenine derivatives, Int. Immunopharmacol. 29 (2) (2015) 354–360.
[25] M. Radu, J. Chernoff, An in vivo assay to test blood vessel permeability, J. Vis. Exp. (73) (2013), e50062.
[26] S. Mishra, et al., Subcutaneous Ehrlich Ascites Carcinoma mice model for studying cancer-induced cardiomyopathy, Sci. Rep. 8 (1) (2018) 5599.
[27] A. Kim, et al., Mouse models of anemia of cancer, PLoS One 9 (3) (2014), e93283.
[28] Dalia S. Morsi, Sobhy Hassab El-Nabi, Mona A. Elmaghraby, Ola A. Abu Ali, Eman Fayad, Shaden A. M. Khalifa, Hesham R. El-Seedi, Islam M. El-Garawani, Anti-proliferative and immunomodulatory potencies of cinnamon oil on Ehrlich ascites carcinoma bearing mice, Sci. Rep.2022 Jul 12;12(1):11839.
[29] S.R. Kabir, et al., Purification and characterization of a Ca(2+)-dependent novel lectin from Nymphaea nouchali tuber with antiproliferative activities, Biosci. Rep. 31 (6) (2011) 465–475.
[30] M. Alshathly, E. Elsharkawy, Inhibition of Ehrlich ascites carcinoma by lactuca serriola in Swiss albino mice, J. Chem. Chem. Eng. 8 (2014) 66–71.
[31] S. Dallakyan, A.J. Olson, Small-molecule library screening by docking with PyRx, Methods Mol. Biol. 1263 (2015) 243–250.
[32] S. Kim, et al., PubChem substance and compound databases, Nucleic Acids Res. 44 (D1) (2016), D1202-13.
[33] N.M. O'Boyle, et al., Open Babel: an open chemical toolbox, J. Cheminf. 3 (2011) 33.
[34] S. Hammami, et al., Isolation and structure elucidation of a flavanone, a flavanone glycoside and vomifoliol from Echiochilon fruticosum growing in Tunisia, Molecules 9 (7) (2004) 602–608.
[35] D. Okin, R. Medzhitov, Evolution of inflammatory diseases, Curr. Biol. 22 (17) (2012), R733-40.
[36] N. Nasim, I.S. Sandeep, S. Mohanty, Plant-derived natural products for drug discovery: current approaches and prospects, Nucleus (Calcutta) 65 (3) (2022) 399–411.
[37] S.R. Shejale, Y. V, C., Phytochemical screening on Champaka pushpam (Michelia champaca), Res. J. Pharm. Technol. 12 (7) (2019) 3541–3546.
[38] K. Karthik, D.K. Kumar, *E*valuation of analgesic, anti-inflammatory of stem bark ethanolic extract of michelia champaca Linn, Asian J. Pharmaceut. Res. 7 (2017) 94.
[39] U. Parimi, D. Kolli, Antibacterial and free radical scavenging activity of Michelia champaca Linn. flower extracts, Free Radic. Antioxidants 2 (2012) 58–61.
[40] H.F. Dvorak, Vascular permeability to plasma, plasma proteins, and cells: an update, Curr. Opin. Hematol. 17 (3) (2010) 225–229.
[41] A. Azab, A. Nassar, A.N. Azab, Anti-inflammatory activity of natural products, Molecules (10) (2016) 21.
[42] Y. Tamrat, et al., Anti-inflammatory and analgesic activities of solvent fractions of the leaves of Moringa stenopetala Bak. (Moringaceae) in mice models, BMC Compl. Alternative Med. 17 (1) (2017) 473.
[43] H. Khan, et al., Glycosides from medicinal plants as potential anticancer agents: emerging trends towards future drugs, Curr. Med. Chem. 26 (13) (2019) 2389–2406.
[44] D.B. Kitchen, et al., Docking and scoring in virtual screening for drug discovery: methods and applications, Nat. Rev. Drug Discov. 3 (11) (2004) 935–949.
[45] M. Zhao, et al., Design, synthesis and biological evaluation of dual Topo II/HDAC inhibitors bearing pyrimido[5,4-b]indole and pyrazolo[3,4-d]pyrimidine motifs, Eur. J. Med. Chem. 252 (2023) 115303.
[46] A.M. Saeed, et al., Anti-cancer activity and molecular docking of some pyrano[3,2-c]quinoline analogues, Open J. Med. Chem. 10.1 (2020) 1–14.
[47] J.J. Perez, C.S. Lupala, P. Gomez-Gutierrez, Designing type II topoisomerase inhibitors: a molecular modeling approach, Curr. Top. Med. Chem. 14 (1) (2014) 40–50.
[48] V.M. Matias-Barrios, X. Dong, The implication of topoisomerase II inhibitors in synthetic lethality for cancer therapy, Pharmaceuticals (Basel) (1) (2023) 16.
[49] C.K. Jain, H.K. Majumder, S. Roychoudhury, Natural compounds as anticancer agents targeting DNA topoisomerases, Curr. Genom. 18 (1) (2017) 75–92.
[50] L. Wang, et al., Quercetin downregulates cyclooxygenase-2 expression and HIF-1α/VEGF signaling-related angiogenesis in a mouse model of abdominal aortic aneurysm, BioMed Res. Int. 2020 (2020) 9485398.
[51] N. Singh, et al., Inflammation and cancer, Ann. Afr. Med. 18 (3) (2019) 121–126.